

Article

Ambient Vibration Analysis of Diversion Pipeline in Mount Changlong Pumped-Storage Power Station

Jijian Lian, Linrui Zuo, Xiaoqun Wang * and Lu Yu

School of Water Conservancy and Hydroelectric Power, Hebei University of Engineering, Handan 056038, China; jjlian@tju.edu.cn (J.L.); zlr2995476678@zohomail.cn (L.Z.); yulu6767@zohomail.cn (L.Y.)

* Correspondence: 1014205052@tju.edu.cn

Abstract: This study analyzes the ambient vibrations induced while running the Mount Changlong pumped-storage power station (PSPS). The ground vibration data of the power station during its operation were acquired with vibration sensors. Different units were selected and compared under working conditions, and the conclusions were as follows: (1) Ambient vibrations induced by the running of units constituted the primary source of vibration, and they attenuated as the distance increased. (2) The vibration acceleration under pumping conditions was larger than that under power generation conditions, and the ground vibration acceleration increased with an augmentation of the power. (3) The running of adjacent units generated mutual interference, and the types of units were different, which led to complex variations in the spectrum maps. (4) The vibration acceleration of the lower flat tunnel was prone to surpassing the standard when the number of units running together exceeded three.

Keywords: pumped-storage power station; ambient monitoring; diversion pipeline; analysis of vibration; vibration standard



Citation: Lian, J.; Zuo, L.; Wang, X.; Yu, L. Ambient Vibration Analysis of Diversion Pipeline in Mount Changlong Pumped-Storage Power Station. *Appl. Sci.* **2024**, *14*, 2196.

<https://doi.org/10.3390/app14052196>

Academic Editor: Mickaël Lallart

Received: 2 February 2024

Revised: 1 March 2024

Accepted: 1 March 2024

Published: 6 March 2024



Copyright: © 2024 by the authors. Licensee MDPI, Basel, Switzerland. This article is an open access article distributed under the terms and conditions of the Creative Commons Attribution (CC BY) license (<https://creativecommons.org/licenses/by/4.0/>).

1. Introduction

Vibrations within the vicinity of both the plant and the diversion pipeline are generated throughout the running phase of a pumped-storage power station due to its inherent features of high head, high speed, and high capacity [1]. Previously, some power stations have caused severe accidents because of these vibrations [2–6], and the incidents resulted in casualties. The influences of vibrations can also give rise to issues for ground architectures and residents.

The vibration sources have been researched in extensive studies. Hydraulic, mechanical, and electrical factors are the main reasons for vibrations while running units [7]. The hydraulic factor is the most crucial of these [8], which mainly results from uneven flow between the guide blades and the runner. The region without blades between the movable guide blades and the runner is referred to as the vaneless area [9]. During the operation of the units, the vaneless area generates multiple overlapping pulsating pressures with a main frequency approximately equal to the passing frequency of the runner blades (referred to as the blade frequency, calculated by multiplying the number of runner blades by the speed frequency) [10]. This high-frequency pressure pulsation is transmitted upstream via the water hammer effect, resulting in vibrations along the pipeline [11].

Researching the propagation of vibration, Rubin analyzed the response of the concrete structure in the steel pipe pressure compensation section of the Degorsk PSPS. The findings demonstrated that incorporating a compensator into the pipe section significantly enhanced its stability, which reduced the vibrations of the diversion pipeline [12]. Masoud Babaei utilized the finite element method to analyze the natural frequencies of functionally graded graphene sheets (GPL) in different distribution modes while considering different material parameters and boundary conditions. The findings revealed that FG-O types exhibited the minimum natural frequencies [13]. Kurzweil investigated the secondary vibration and

noise of the surrounding ground induced by high-speed trains and analyzed the law of vibration propagation in different soil layers [14]. Hoods proposed a comprehensive set of calculation methods and an evaluation standard for assessing railway ground vibrations and noise, which can also be utilized for the ground vibration of PSPSs [15].

The problem of vibration necessitates the implementation of vibration reduction measures. Chen utilized finite element software to simulate the cushion pipeline thickness and elastic modulus of a diversion pipeline. The results demonstrated that increasing the cushion pipeline thickness while decreasing the elastic modulus achieved better vibration reduction effects [16]. Xu researched the global collapse resistance capacity of a seismic-damaged steel-reinforced concrete (SRC) frame structure strengthened with an enveloped steel jacket. The results demonstrated the ability of the enveloped steel jacket reinforcement to effectively enhance the SRC frame structure's resistance to global collapse. It is also valuable for the vibrations of diversion pipelines [17]. Dincer used the characteristic line method and software to research the impact of the presence of a surge chamber on hydraulic transients under diverse working conditions, concluding that implementing a surge chamber can effectively mitigate the occurrence of cavitation [18]. Jalut utilized MATLAB to numerically simulate the control equation of transient flow in a pipeline with or without a surge chamber. The results demonstrated the effectiveness of the surge chamber in regulating the pressure along the pipeline, and the vibration level was significantly diminished [19].

Although there are studies on the law of vibration propagation, research regarding ground analysis and vibration in the diversion pipeline areas of PSPSs is lacking. Most studies are limited to numerical simulations and analyzing the vibration frequency. However, studying the propagation law and magnitude of vibrations during the transmission of vibrations from the diversion pipeline to the ground under different conditions is crucial. This can significantly mitigate the limitations of numerical simulations and play an important role in the construction of PSPSs. This paper innovatively utilizes the Mount Changlong PSPS as an example, analyzing the ambient vibrations related to diversion pipelines based on measured data, and providing valuable guidance for the future construction of PSPSs.

2. Research Object and Test Arrangement

2.1. Research Object

The Mount Changlong PSPS is situated in Tianhuangping Town, Anji County, Zhejiang Province. It is the largest PSPS in East China, boasting a maximum generating head of 756.5 m. The pivotal structure of the power station comprises the upper reservoir, lower reservoir, water conveyance system, underground plant cavern group, and ground switching station. The water conveyance system is designed with three tunnels and six machines, and the lengths of each pipeline range from 2738.1 to 2810.3 m. It accommodates six generator units equipped with mixed-flow reversible-pump turbine generators rated at 350 MW each, resulting in a total installed capacity of 2100 MW (6×350 MW). Figure 1 shows an aerial view and the partial facility of the PSPS (refer to Table 1 for the basic parameters, the first unit is designated as 1# and so on). We carried out vibration monitoring for nine days to obtain ambient vibration data on the diversion pipeline during the power station's operation.

Table 1. The fundamental parameters of units.

Pump Turbine			Generator Motor		
Argument	Unit	Remark	Argument	Unit	Remark
Number of runner blades	-	10 (1#–4#), 11 (5#; 6#)	Rated power	MW	389 MW / 350 MW
Rated power	MW	357	Rated speed	r/min	500 (1#–4#), 600 (5#; 6#)



Figure 1. The top view and facility of the PSPS.

2.2. Setting of the Measuring Points

The test focused on the diversion pipeline area of the Mount Changlong PSPS. The principles for arranging the measurement points were as follows: ① In the diversion pipeline area, it was important to cover as many pipeline sections along the diversion pipeline as possible. Additionally, suitable locations needed to be selected to arrange monitoring points with intervals of 50 m or 100 m perpendicular to the direction of the pipeline. This facilitated the subsequent analysis of vibration propagation and ensured rationality in the analysis. If there were changes in the diversion pipeline material or cross-section, or if faults existed in the mountainous region, emphasis needed to be placed on testing in those areas. ② Within the plant area, the measurement points needed to be positioned near the units and related equipment, with appropriate protective measures implemented for this region. ③ Vibration mainly affects residential areas; therefore, relevant measurement points needed to be arranged accordingly.

The measurement points were positioned within the designated areas of the power station according to the description provided in the relevant geological data (please refer to Table 2 and Figure 2 for a detailed illustration of their specific arrangement). All measurement points were equipped with vibration acceleration sensors, and the sampling frequency was 8000 Hz.

Table 2. Positioning of the measure points.

No.	Name	Remark	No.	Name	Remark
1	P1	Upper reservoir	5	P5	Near units 3# and 4#
2	P2		6	P6	Near units 5# and 6#
3	P3	The measurement points near the horizontal flat tunnel were influenced by cars.	7	P7	The measurement points near the horizontal flat tunnel were influenced by construction.
4	P4		8	P8	
			9	P9	Lower flat tunnel

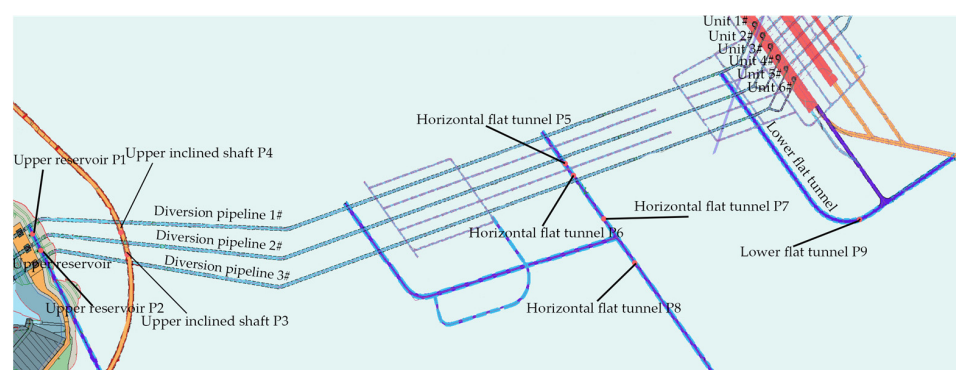


Figure 2. Overview of measurement point locations.

2.3. Vibration Inducement

Five fundamental conditions (shutdown, power generation and phase control, the operation of power generation, pumped storage, and pumped phase control), along with twelve specific conditions, feature in the running process of a PSPS. The transitions between these conditions can result in increased vibrations within the power station structure. Theoretically, no vibrations occur in shutdown conditions; therefore, units 1#, 2#, 3#, 4#, and 5# in pumping conditions were compared with shutdown conditions.

Before the test, this study primarily concentrated on the propagation of z-direction vibrations. The presence of horizontal vibrations was inconsequential. A portable vibration calibrator was utilized to calibrate the acceleration sensor to reduce the experimental error as much as possible. In the data analysis, the digital filter of Butterworth was utilized to filter the signal. The order of the filter was four, to maximize the fidelity of the detected signal. The critical frequency was 0.5. The filter utilized was a low-pass filter. And the measured data were processed using the detrend function to remove data trend items and reduce external ambient interference. Subsequently, the z-direction vibration acceleration spectrum maps and root mean of vibration were obtained for each measuring point, as shown in Figures 3 and 4. The specific working conditions are shown in Table 3. The power generation conditions required a power higher than 0 MW, and the pumping conditions required a power lower than 0 MW.

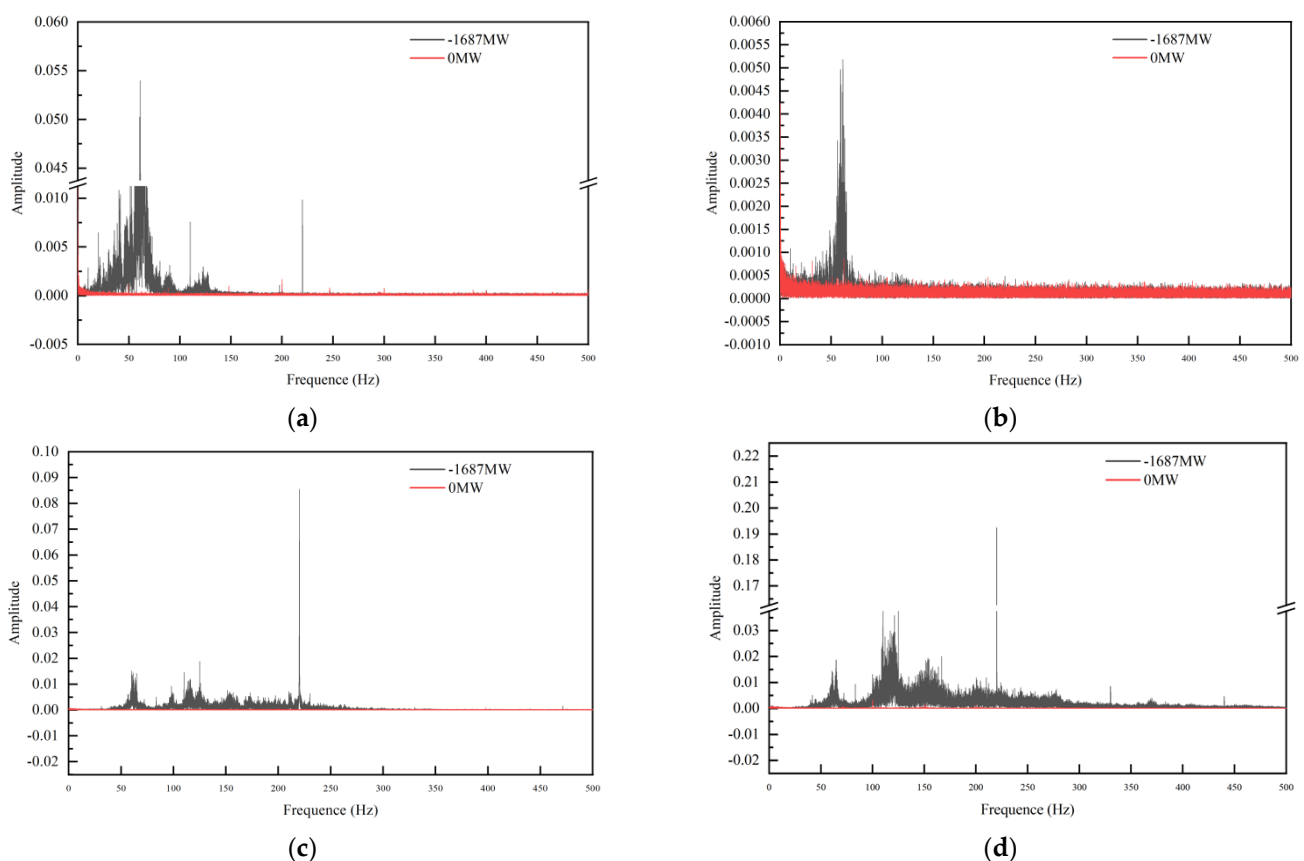


Figure 3. The spectrum maps of shutdown conditions and five units in pumping conditions. (a) P1—upper reservoir; (b) P3—upper inclined shaft; (c) P8—horizontal flat tunnel; (d) P9—lower flat tunnel.

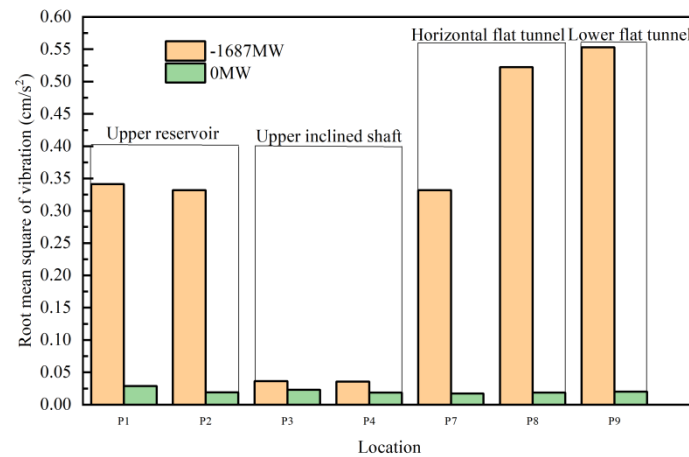


Figure 4. The root–mean of vibration values of units 1#, 2#, 3#, 4#, and 5# in pumping and shutdown conditions.

Table 3. Shutdown conditions and five units under pumping conditions.

Conditions	Power (MW)
Shutdown conditions	0
Units 1#, 2#, 3#, 4#, and 5# under pumping conditions	–1650

The above results indicate that the amplitude of the z-direction vibration of each measuring point was negligible under shutdown conditions. The spectrum maps resemble white noise. Under pumping conditions, however, the amplitude of the z-direction vibration at each measuring point significantly increased compared with shutdown conditions. Moreover, a dominant frequency emerges near 70 Hz in the spectrum maps. This comparison proves that ambient vibration was generated during the operation of the units and had an impact on the ground. The subsequent analysis depended on this conclusion.

As shown in Figure 4, the root–mean of vibration of each measuring point in the five units while running significantly changed compared with the shutdown conditions, proving the conclusion regarding the spectrum maps. Analyzing the shutdown condition revealed an ambient vibration of approximately 0.02 cm/s² in the whole division pipeline area, and this did not affect the daily lives of nearby residents.

3. Ambient Vibration Analysis

3.1. Research on Vibration under Power Generation and Pumping Conditions

The above research indicates that the ground vibration significantly changed under pumping conditions compared with shutdown conditions. Based on this, there may be discrepancies in the ground vibration between the power generation and pumping conditions. Therefore, the spectrum maps and root–mean of vibration diagrams of unit 4# and units 1# and 3# under power generation and pumping conditions were selected for investigation. The running powers of unit 4# and units 1# and 3# are shown in Table 4. The analysis results are shown in Figures 5–8.

Table 4. Powers of unit 4# and units 1# and 3# under power generation and pumping conditions.

Conditions	Power (MW)
Unit 4# under power generation conditions	350
Unit 4# under pumping conditions	–344
Units 1# and 3# under power generation conditions	697
Units 1# and 3# under pumping conditions	–657

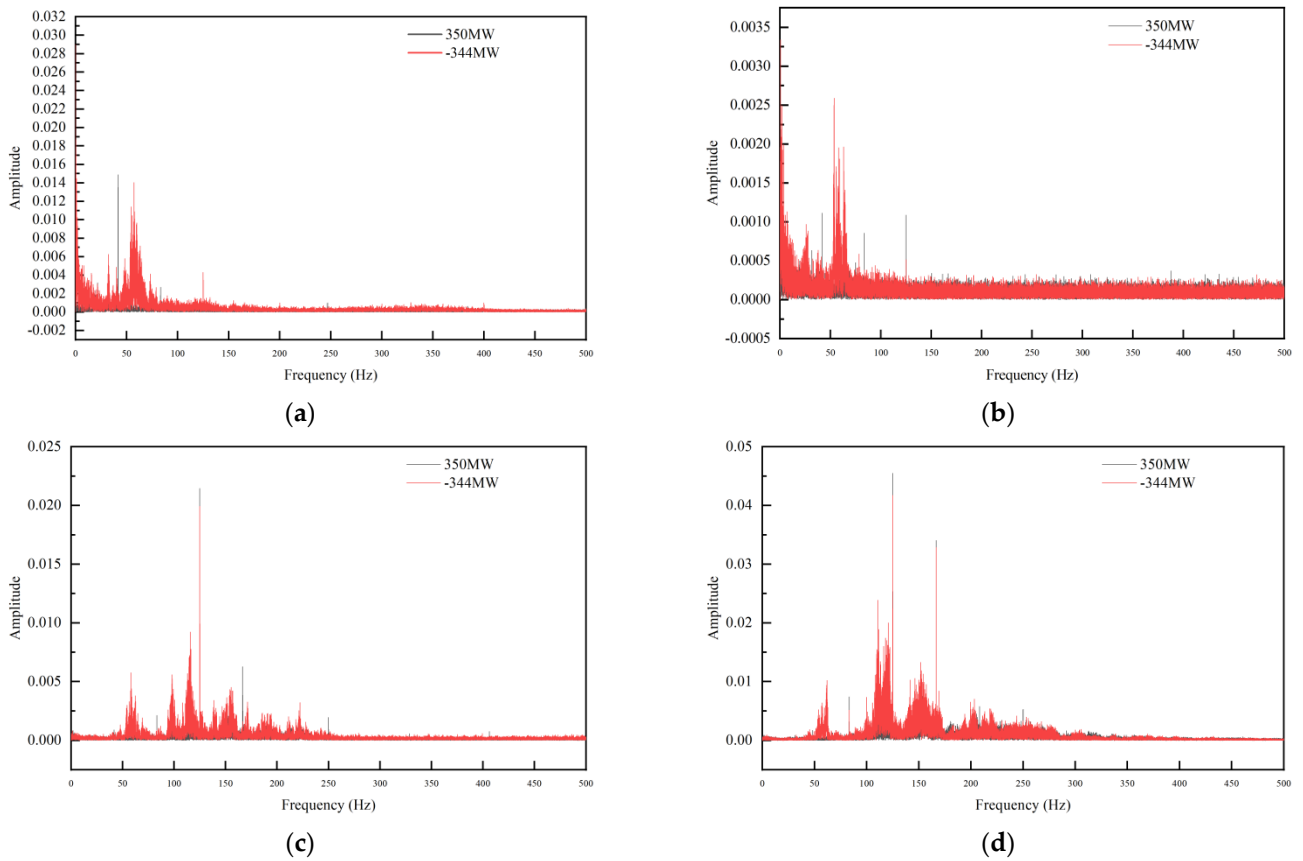


Figure 5. The spectrum maps of unit 4# under power generation and pumping conditions. (a) P1—upper reservoir; (b) P4—upper inclined shaft; (c) P8—horizontal flat tunnel; (d) P9—lower flat tunnel.

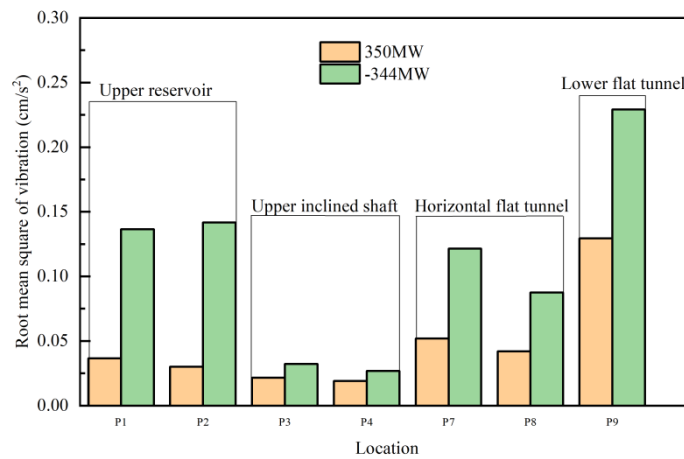


Figure 6. The root-mean of vibration of unit 4# under power generation and pumping conditions.

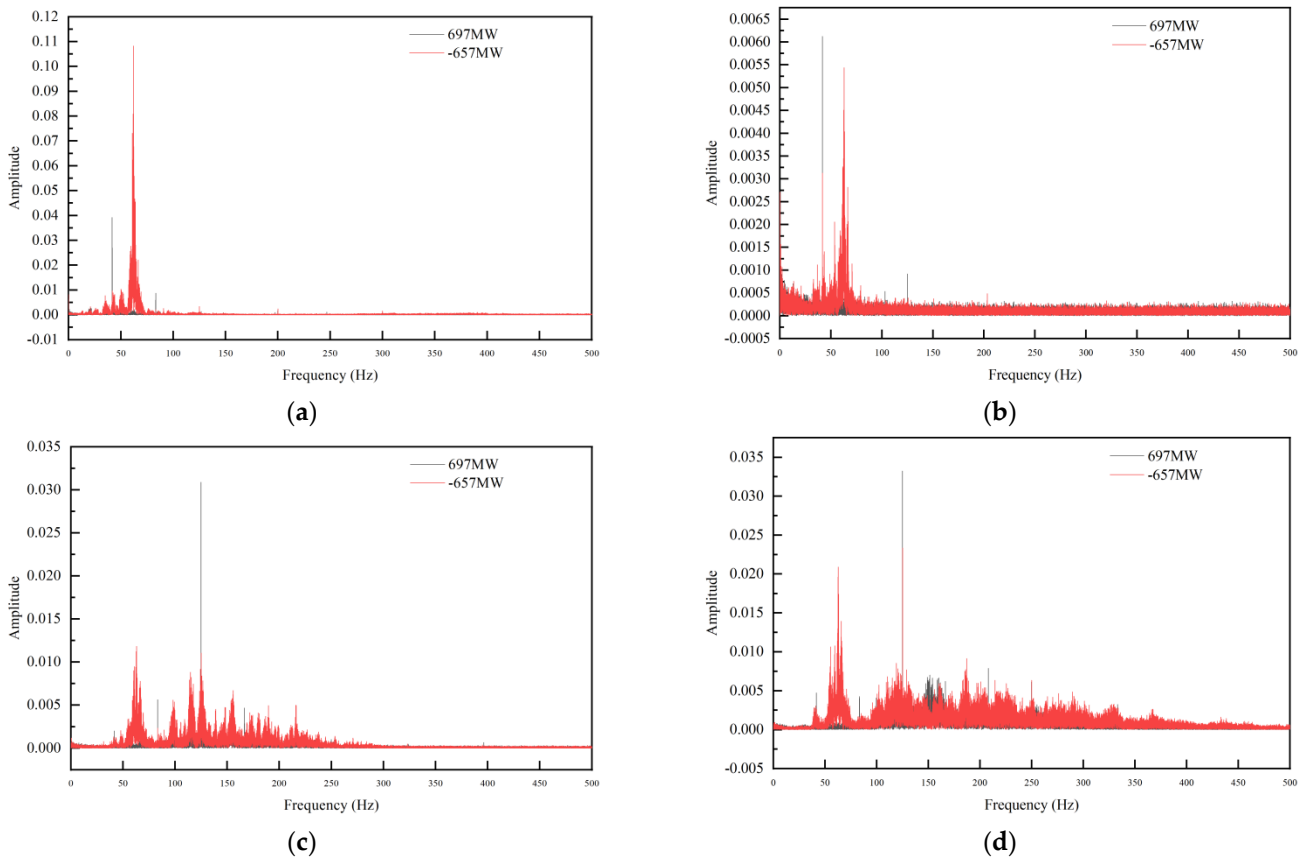


Figure 7. The spectrum maps of units 1# and 3# under power generation and pumping conditions. (a) P1—upper reservoir; (b) P4—upper inclined shaft; (c) P8—horizontal flat tunnel; (d) P9—lower flat tunnel.

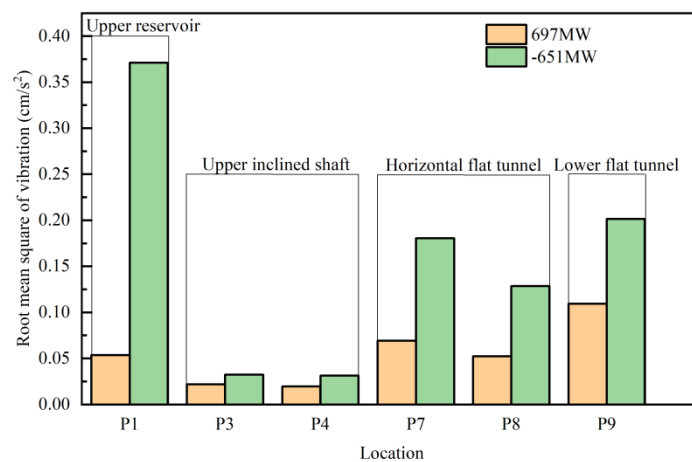


Figure 8. The root–mean of vibration in units 1# and 3# under power generation and pumping conditions.

In the spectrum maps of unit 4# in Figure 5, the amplitudes of the upper reservoir, the horizontal flat tunnel, and the lower flat tunnel exhibit significant magnitudes, whereas the amplitude of the upper inclined shaft is smaller. Within 100 Hz, the energy is primarily concentrated at 60 Hz and 70 Hz. From 100 Hz to 200 Hz, the energy is primarily concentrated at 120 Hz and 170 Hz. The spectrum map values for the pumping condition exceed those for the power generation condition.

The results of the root–mean of vibration in Figure 6 validate the results depicted in the spectrum maps, such that the root–mean of vibration was higher in pumping conditions

than in power generation conditions. Furthermore, the vibrations originated from the plant and the units and propagated outward, therefore these two locations with greater vibrations were close to the upper reservoir and the lower flat tunnel. The root-mean of vibration in the inner sections of the diversion pipeline gradually diminished as the distance increased. The maximum values of the root-mean of vibration were 0.13 cm/s^2 and 0.22 cm/s^2 in the lower flat tunnel, and the minimum values of the root-mean of vibration were 0.02 cm/s^2 and 0.03 cm/s^2 in the horizontal flat tunnel. There was no discrepancy compared with the background noise, so it was disregarded.

As shown in Figure 7, the amplitude of the upper reservoir was much higher than that of the other measuring points because the measuring point of the upper reservoir was near both the reservoir and the factory buildings, and the testing process may have been influenced by an inevitable external interference. Compared with the other measuring points, the law of amplitude was the same as when unit 4# was running. Within 100 Hz, the energy was primarily concentrated at 60 Hz and 70 Hz. From 100 to 200 Hz, the energy was primarily concentrated at 120 Hz and 160 Hz.

Based on Figure 8, the maximum values of the root-mean of vibration were 0.1 cm/s^2 and 0.2 cm/s^2 in the lower flat tunnel. The minimum values of the root mean of vibration were 0.02 cm/s^2 and 0.03 cm/s^2 in the horizontal flat tunnel. The other flaws were the same as unit 4# was running, so the specific description will not be elaborated on in this context.

3.2. Research on the Effect of Power Increase on Vibration

Based on actual requirements, the running of a PSPS often necessitates the simultaneous functioning of multiple units, which means that multiple units collaborate under power generation conditions or pumping conditions. The z-direction vibration acceleration in each section of the diversion pipeline undergoes variations with the increase in the number of units running. This section mainly researches the variation with the increase in power. The main working conditions are shown in Tables 5 and 6. The analysis results are shown in Figures 9 and 10.

As shown in Figure 9, the root-mean of vibration at each measuring point increased with increasing power under power generation conditions. The measuring point in the lower flat tunnel obtained a maximum value of 0.54 cm/s^2 . Moreover, the upper inclined shaft obtained a minimum value, and the vibration energy was attenuated by approximately 90% when it reached this measuring point. At this time, there was no discrepancy in the root-mean of vibration compared with shutdown conditions, indicating that the upper inclined shaft location was unaffected by vibration. Therefore, the vibration in this part was negligible.

As shown in Figure 10, the propagation law under pumping conditions resembled that under power generation conditions with increasing power. The largest root-mean of vibration occurred in the lower flat tunnel, with a value of 0.55 cm/s^2 at -1687 MW , and it decreased rapidly with increasing distance. Considering the measuring point of the upper reservoir, the pumping condition exhibited discrepancies compared with the power generation condition. The maximum root mean of vibration did not exceed 0.1 cm/s^2 in power generation conditions; on the contrary, the minimum root mean of vibration was close to 0.15 cm/s^2 . This shows that the upper reservoir was affected more under pumping conditions. The vibration acceleration of the upper inclined shaft remained relatively stable.

Table 5. Power generation working conditions.

Conditions	Power (MW)
Unit 4# under power generation conditions	350
Units 1# and 3# under power generation conditions	700
Units 1#, 4#, and 5# under power generation conditions	1050

Table 6. Pumping working conditions.

Conditions	Power (MW)
Unit 4# under pumping conditions	−344
Units 1# and 4# under pumping conditions	−651
Units 1#, 3#, and 4# under pumping conditions	−980
Units 1#, 2#, 4#, and 5# under pumping conditions	−1384
Units 1#, 2#, 3#, 4#, and 5# under pumping conditions	−1687

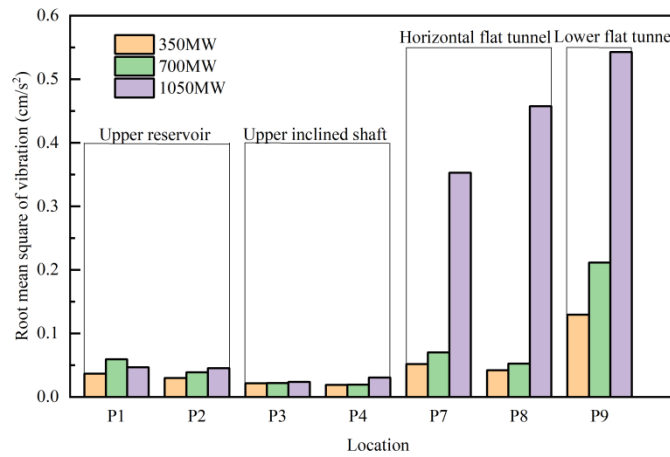


Figure 9. Variation in the root–mean of vibration with power under power generation conditions.

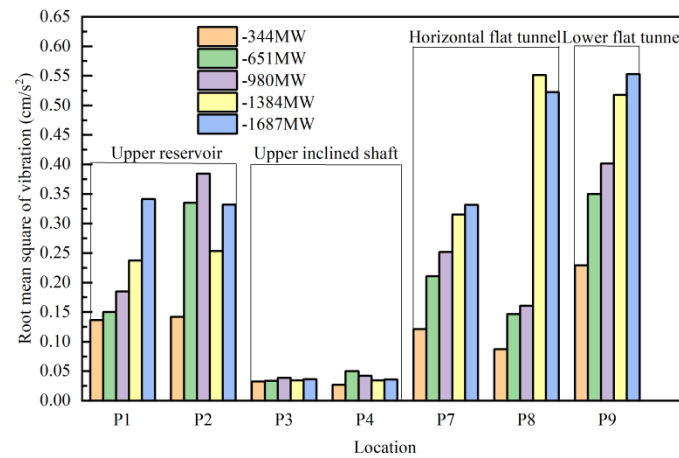


Figure 10. The variation in the root–mean of vibration with power under pumping conditions.

3.3. Research on Pipeline Vibration

Two measurement points, P5 and P6, were set directly above the diversion pipeline. Previous studies researched the ambient vibration in the ground, and the ground vibration was generated by the vibration of the diversion pipeline via the mountains. Therefore, the extent to which the vibration of the diversion pipeline diminishes after the vibration reaches the ground is significant to study.

As depicted in Figure 11, a small section of exposed steel lining in the latter half of the horizontal flat tunnel section of the diversion pipeline of the PSPS facilitated maintenance. This section could be accessed through the construction branch of 3#. Measuring points P5 and P6 within the horizontal flat tunnel were directly connected to diversion pipelines 2# and 3#, experiencing negligible external interference. Additionally, units 1# and 2# shared the same diversion pipeline of 1#, units 3# and 4# shared another diversion pipeline of 2#, and units 5# and 6# shared another diversion pipeline of 3#. The collected data during testing originated solely from vibrations generated by these diversion pipelines while running the units. This section researches the law of vibration acceleration in the diversion pipeline with the increase in the number of units running under different conditions. The working conditions are shown in Table 7.

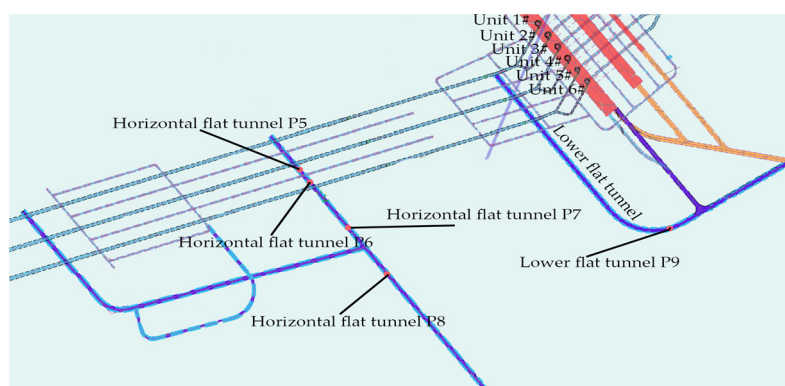


Figure 11. Position diagram of measuring points in the horizontal flat tunnel.

Table 7. Working conditions.

Conditions	Power (MW)
Units 1# and 4# under power generation conditions	350
Units 1#, 4#, and 5# under power generation conditions	1050
Units 1#, 3#, 4#, and 5# under pumping conditions	−1380

As shown in Figure 12, the amplitudes of measuring points P5 and P6 were larger than the others. Under sectional conditions, the amplitude reached 35, indicating that the energy was greatly weakened from the diversion pipeline to the ground compared with the ground vibration. Compared with the other spectrum maps of the working conditions, the energy was predominantly concentrated around 70 Hz and 120 Hz in the majority of working conditions.

Based on Figure 13, measurement point P6 in units 1# and 4# generated a root-mean of vibration of approximately 0.68 cm/s^2 while running the diversion pipeline of 2# under power generation conditions. The diversion pipeline of 3# was not running at that time. Based on this phenomenon, mutual interference occurred while running the adjacent pipelines. Moreover, the root-mean of vibration increased with the increasing number of units in operation, with a maximum value of 76 cm/s^2 . The presence of mountains significantly attenuated the magnitude of vibrations. The ground vibration was caused by the vibration of the diversion pipeline.

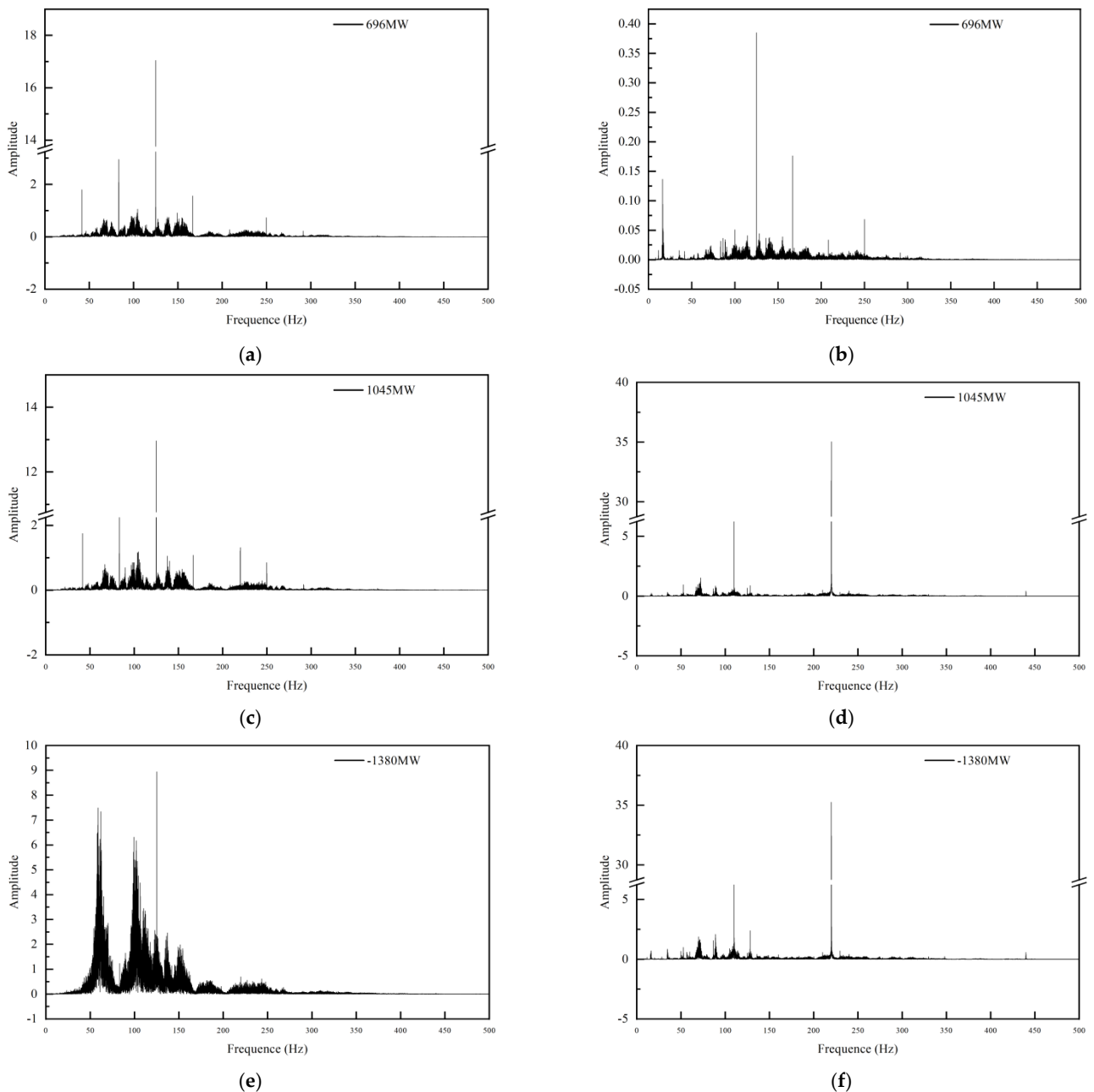


Figure 12. The spectrum maps of units 1# and 4# and units 1#, 4#, and 5# under power generation conditions, and units 1#, 3#, 4#, and 5# in pumping conditions. (a) P5—units 1# and 4# under power generation conditions; (b) P6—units 1# and 4# under power generation conditions; (c) P5—units 1#, 4#, and 5# under power generation conditions; (d) P6—units 1#, 4#, and 5# under power generation conditions; (e) P5—units 1#, 3#, 4#, and 5# under pumping conditions; (f) P6—units 1#, 3#, 4#, and 5# under pumping conditions.

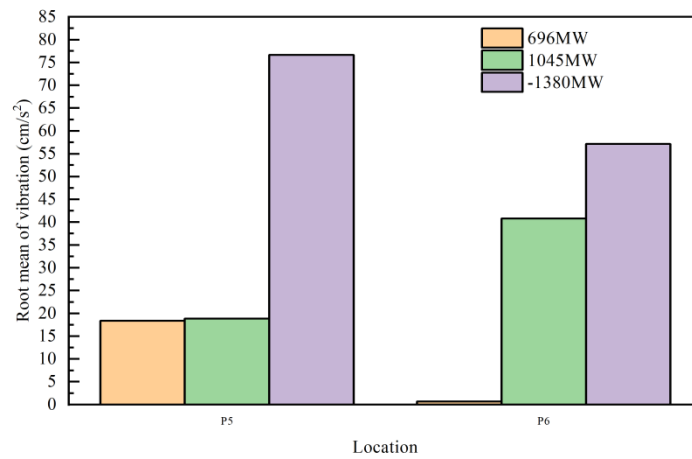


Figure 13. The root-mean of vibration of units 1# and 4# and units 1#, 4#, and 5# under power generation conditions, and units 1#, 3#, 4#, and 5# under pumping conditions.

3.4. Research on the Influence of Unit Type on Vibration

We learned the units of the power station were manufactured by two companies and the types of units were different during our investigation. The data indicate that the main discrepancies between them were in the number of blades and the rated speed. Units 1#, 2#, 3#, and 4# were equipped with five long blades and five short blades, corresponding to sixteen movable guide blades. The rotational speed of these units was set at 500 r/min. Units 5# and 6# were equipped with 11 blades and 20 movable guide blades. The rotational speed was set at 600 r/min.

We selected some of the working conditions for analysis for these two types of units. The running conditions are presented in Table 8. The analysis results are shown in Figures 14 and 15.

Table 8. Power generation working conditions of two units.

Conditions	Power (MW)
Units 1# and 4# under power generation conditions	696
Units 1# and 5# under power generation conditions	697

As shown in Figure 14, the amplitude was concentrated at 220 Hz in units 1# and 5# under power generation conditions. Meanwhile, the amplitude was concentrated at 120 Hz in units 1# and 4# under power generation conditions, indicating the energy was higher in unit 5# than in unit 4#.

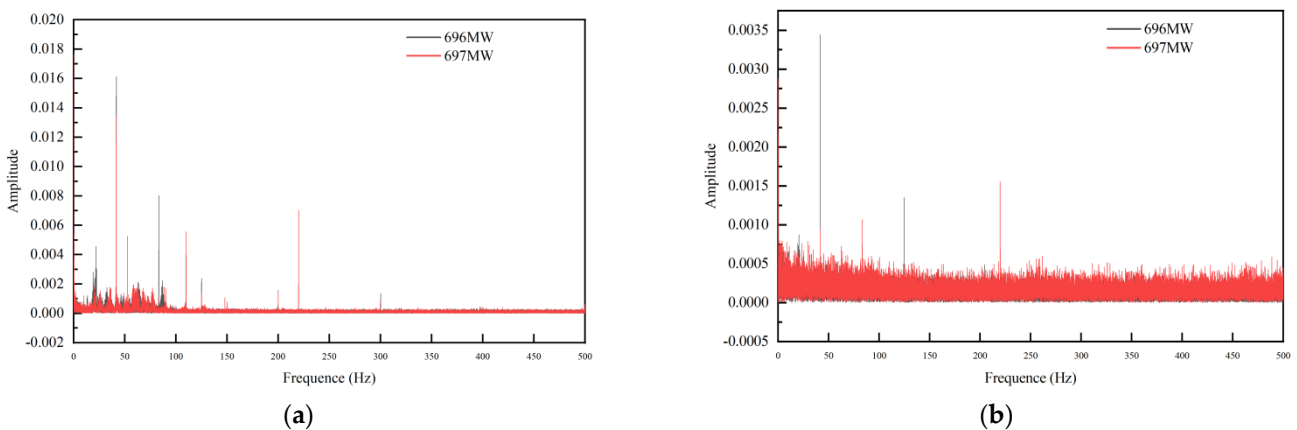


Figure 14. Cont.

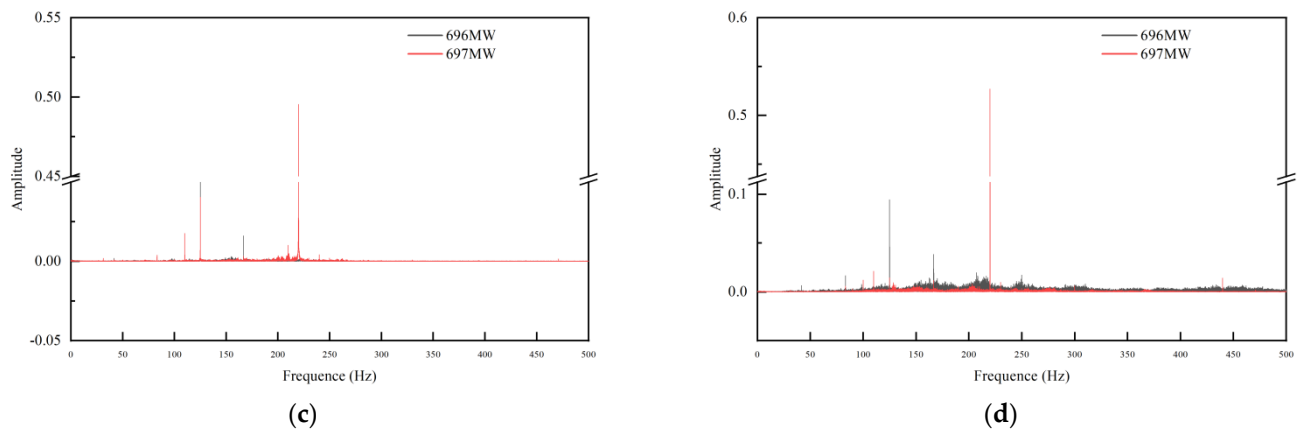


Figure 14. The spectrum maps of units 1# and 4#, and units 1# and 5# under power generation conditions. (a) P1—upper reservoir; (b) P3—upper inclined shaft; (c) P8—horizontal flat tunnel; (d) P11—lower flat tunnel.

Based on Figure 15, the acceleration of the vibration of units 1# and 5# was higher than that of units 1# and 4#. In conclusion, the results show that the different types of units significantly influenced the vibration of the diversion pipeline. This result may be due to the rotational speed and the number of guide blades, whereby faster speeds tend to require more energy to maintain. Therefore, the vibration was higher.

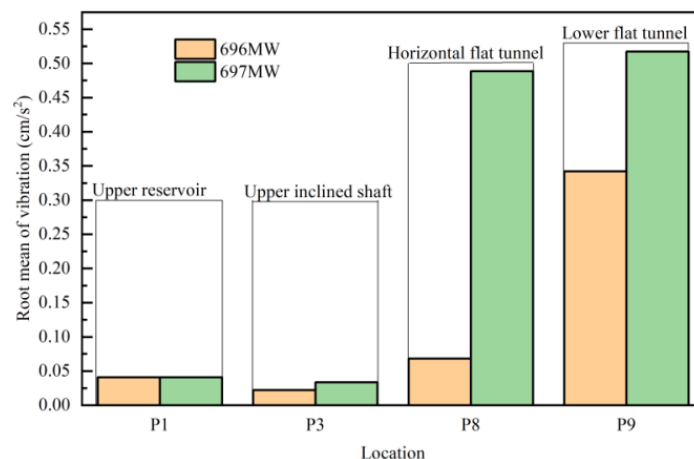


Figure 15. The root mean of vibration of units 1# and 4#, and units 1# and 5# under power generation conditions.

4. Frequency Analysis and Vibration Evaluation

4.1. Analysis of Vibration Frequency

We carried out a brief analysis of the frequencies with relatively concentrated energy in the spectrum maps. However, the origin of these frequencies remained unknown, so the question was further analyzed.

According to relevant research findings, pressure pulsations generated within the vaneless area predominantly propagate upstream as pressure waves while running the units. These pressure pulsations primarily correspond to the passing frequency of the water pump turbine runner blades, with a majority exhibiting dominant frequencies that are integer multiples of the lobe frequency. The specific calculation formula for this phenomenon is as follows:

$$f = \frac{n_H \times Z_1}{60} K, K = 1, 2 \quad (1)$$

where f is the primary frequency. The rotational speed of the units, denoted as n_H , was a crucial parameter in this study. Z_1 represents the number of rotor blades, and K is the integer coefficient of the ratio of rotor blades to guide blades [20], which is rounded off to obtain the value of K .

The frequencies for units 1#, 2#, 3#, and 4# were

$$f_1 = 83.33 \text{ (Hz)}, f_2 = 166.67 \text{ (HZ)} \quad (2)$$

For units 5# and 6#, the frequencies were

$$f_3 = 110 \text{ (Hz)}, f_4 = 220 \text{ (Hz)} \quad (3)$$

In these results, the frequency was within 100 Hz, and the energy was primarily concentrated at 60 Hz and 70 Hz. From 100 Hz to 200 Hz, the energy was primarily concentrated at 120 Hz and 170 Hz, whereas the energy in units 5# and 6# was concentrated at 220 Hz. These frequencies were different from the previous results. Based on the conclusions in Sections 3.3 and 3.4, there was mutual interference while running adjacent pipelines and some discrepancies between different types of units. We suspect this is why the test results were inconsistent with the theoretical calculation results. To prove this conclusion, we recommend setting up measuring points in the volute to directly measure the frequencies in the units which were running.

4.2. The Evaluation of Vibration

The vibration in the area of the diversion pipeline has been analyzed. However, there is currently no globally unified standard for evaluating ambient vibration and noise. The research on vibration and noise in this area primarily relies on urban area noise and vibration standards. The ambient vibration control standard for the diversion pipelines of PSPSs is mainly based on GB1007-88 [21]. Table 9 presents the standard values of Z-direction vibrations in various urban areas.

Table 9. Vertical vibration standards in different urban areas.

The Application Scope	Daytime (dB)	Nighttime (dB)
Special residential area	65	65
Residential, cultural, and educational areas	70	67
Mixed and central business areas	75	72
Industrial concentration area	75	72
Both sides of the traffic trunk road	75	72
Both sides of the main railway line	80	80

According to the regional characteristics of PSPSs, the vibration standards for residential, cultural, and educational areas are applied in these zones, while partial areas adopt the vibration standards for mixed areas (a “mixed area” refers to a general commercial and residential area or an industrial, commercial, light-traffic, and mixed residential area). The vibration acceleration level is defined as 20 times the logarithm base 10 of the acceleration–base acceleration ratio, expressed as VAL . The specific formula is as follows:

$$VAL = 20 \lg \frac{a}{a_0} \text{ (dB)} \quad (4)$$

where ‘ a ’ is the effective value of vibration acceleration and $a_0 = 10^{-6} \text{ m/s}^2$ is the base acceleration.

According to the vertical vibration standards for various urban areas, the daytime vibrations in the diversion pipeline area should not exceed 70 dB (0.316 cm/s^2), while the nighttime vibration should not exceed 67 dB (0.224 cm/s^2). The vibrations in specific

regions should not exceed 75 dB (0.562 cm/s^2) during the daytime and 72 dB (0.398 cm/s^2) at nighttime.

Combining these data with the test data, the vibration of the lower flat tunnel was prone to exceeding the standard, especially if the number of units running together exceeded three. For this reason, the initial phase of the construction of the lower flat tunnels was situated within mountainous regions to reduce the influence on the ground. The vibration acceleration of the other measuring points generally fell within an acceptable range.

5. Conclusions

Regarding the ambient vibration of the diversion pipeline of the PSPS, this research focused on whether the vibration of the ground exceeded the standard. The ground vibration acceleration varied under different working conditions and in different types of units.

The conclusions are as follows:

- (1) Ambient vibrations induced by the running of units constituted the primary source of vibration. The vibration of the diversion pipeline reached up to 76 cm/s^2 when the units were running, and the presence of mountains significantly attenuated the magnitude of vibrations. Meanwhile, a vibration acceleration of approximately 0.02 cm/s^2 was measured in the diversion pipeline area when no units were running.
- (2) The research on the ground vibrations showed that the vibration acceleration under pumping conditions was larger than that under power generation conditions. The ground vibration acceleration increased with the augmentation in power, irrespective of the power generation or pumping conditions. The ground vibration acceleration attenuated as the distance increased. The vibration of the lower flat tunnel was the largest, and the vibration of the upper inclined shaft was the smallest.
- (3) Within 100 Hz, the energy was primarily concentrated at 60 Hz and 70 Hz. From 100 to 200 Hz, the energy was primarily concentrated at 120 Hz and 170 Hz. From 200 to 300 Hz, the energy was primarily concentrated at 220 Hz. The theoretical calculation results were 83.33 Hz and 166.67 Hz for units 1#–4#, and 110 Hz and 220 Hz for units 5# and 6#. The test results were inconsistent with the theoretical calculation results due to mutual interference while running adjacent units and the different types of units, which led to a bias.
- (4) Compared to the existing urban vibration standards, the daytime vibrations in the area of the diversion pipeline should not exceed 70 dB (0.316 cm/s^2), while the nighttime vibrations should not exceed 67 dB (0.224 cm/s^2). The vibrations in specific regions should not exceed 75 dB (0.562 cm/s^2) during the daytime and 72 dB (0.398 cm/s^2) at nighttime. The vibrations of the lower flat tunnel is prone to exceed the standard, especially if the number of units running together exceeds three.

A prototype observation method was employed in this study to monitor the ground vibration while running a PSPS. The researchers emphasized the analysis of ground vibrations in the diversion pipeline to compare with the traditional methods of monitoring plant vibrations. The prototype observation method is worth popularizing to research the vibration issue in the diversion pipeline area of a PSPS. It can reveal the inherent characteristics and propagation laws of vibration. Furthermore, the results will be helpful for future construction of PSPSs. Combining prototype observations and physical model testing may serve as a better method for research in the future and could significantly enhance the reliability of physical model testing.

Author Contributions: Resources, J.L.; writing—original draft preparation, L.Z.; writing—review and editing, X.W.; investigation, L.Y. All authors have read and agreed to the published version of the manuscript.

Funding: This research was supported by the Hebei Natural Science Foundation (grant No. E2023402015) and the National Natural Science Foundation of China (grant No. U21A20164 and U20A20316).

Data Availability Statement: The data presented in this study are available on request from the corresponding author. The data are not publicly available due to privacy.

Conflicts of Interest: The authors declare no conflicts of interest.

References

1. *Basic Terminology of Pumped Storage Power Station*; State Administration for Market Supervision and Administration; Standardization Administration of China: Beijing, China, 2018.
2. Xue, J.; Duan, Z.; Qin, Y. Cause analysis of structural cracks in a factory building of Guangzhou pumped storage power station. *Guangdong Water Resour. Hydropower* **2017**, *12*, 22–26.
3. Peng, T. Vibration monitoring of underground powerhouse structure of Shisanling pumped storage power station. *Hydropower Autom. Dam Monit.* **2005**, *5*, 49–52.
4. Lin, Z. The accident analysis of the pressure steel pipeline in Yanfeng hydropower Station and the detrimental effects of hydraulic vibration are examined. *Guangdong Hydropower Technol.* **1988**, *45–47*, 45–47.
5. Gally, M.; Güney, M.; Rieutord, E. An Investigation of Pressure Transients in Viscoelastic Pipes. *J. Fluids Eng.* **1979**, *101*, 495–499. [[CrossRef](#)]
6. Jaeger, C. The Theory of Resonance in Hydropower Systems. Discussion of Incidents and Accidents Occurring in Pressure Systems. *J. Fluids Eng.* **1963**, *85*, 631–640. [[CrossRef](#)]
7. Cui, Q. Vibration Testing and Analysis of the Underground Structure of a Large Pumped Storage Power Station. Ph.D. Thesis, Wuhan University, Wuhan, China, 2019.
8. Chen, J.; Wang, F.; Ma, Z. Vibration response analysis of the underground structure in a large pumped storage power station. *J. Water Resour. Archit. Engine* **2013**, *11*, 78–81.
9. Li, J.; Zhang, W.; Zhu, B.; Li, Z.; Zhang, F. Study on Pressure Fluctuation in Vaneless Space of Pump-Turbine. *J. Eng. Thermophilic* **2021**, *42*, 1213–1223.
10. Lian, J.; Wang, H.; Qin, L. *The Research Focuses on the Structural Design of a Hydropower Station*; China Water & Power Press: Beijing, China, 2007.
11. Yang, X.; Lian, J.; Zhang, Z.; Zeng, Y. Theoretical analysis of the attenuation characteristics of high, frequency pressure vibration in pumped storage power station. *J. Energy Storage* **2023**, *72*, 108341. [[CrossRef](#)]
12. Rubin, O.D.; Il'in, Y.A.; Lisichkin, S.E.; Nefedov, A.V.; Rozanova, N.V.; Chernenko, V.N. Evaluation of the Stress-Strain State and Strength of Reinforced-Concrete Structures of Compensation Sections in the Penstocks of the Zagorsk Pumped-Storage Power Plant. *Power Technol. Eng.* **2001**, *35*, 458–462.
13. Babaei, M.; Kiarasi, F.; Tehrani, M.S.; Hamzei, A.; Mohtarami, E.; Asemi, K. Three dimensional free vibration analysis of functionally graded graphene reinforced composite laminated cylindrical panel. *Proc. Inst. Mech. Eng. Part L J. Mater. Des. Appl.* **2022**, *236*, 1501–1514. [[CrossRef](#)]
14. Kurzweil, L.G. Ground-borne noise and vibration from underground rail systems. *J. Sound Vib.* **1979**, *66*, 363–370. [[CrossRef](#)]
15. Hood, R.A.; Greer, R.J.; Breslin, M.; Williams, P.R. The calculation and assessment of ground-borne noise and perceptible vibration from trains in tunnels. *J. Sound Vib.* **1996**, *193*, 215–225. [[CrossRef](#)]
16. Chen, J. The Present Study Focuses on Investigating the Vibration Characteristics of Water Diversion Pipelines in Pumped Storage Power Stations. Master's Thesis, Tianjin University, Tianjin, China, 2022.
17. Xu, C.; Guo, C.; Xu, Q.; Yang, Z. The global collapse resistance capacity of a seismic-damaged SRC frame strengthened with an enveloped steel jacket. *Structures* **2021**, *33*, 3433–3442. [[CrossRef](#)]
18. Ali, D.; Zafer, B. Investigation of Waterhammer Problems in Wind-Hydro Hybrid Power Plants. *Arab. J. Sci. Eng.* **2016**, *41*, 4787–4798.
19. Jalut, Q.H.; Rasheed, N.J. Surge Tank Analysis for Water Hammer Remedy for Long Distance Pipeline. *Diyala J. Eng. Sci.* **2018**, *11*, 47–53.
20. Wang, W.; Xu, H.; Liao, C.; An, X. Study on source of strong vibration with multiple passing-frequency of blade in pumped storage hydropower plant. *Water Resour. Hydropower Eng.* **2021**, *52*, 132–142.
21. GB 10070,1988; Standard of Vibration in Urban Area Ambient. State Ambiental Protection Agency: Beijing, China, 1988.

Disclaimer/Publisher's Note: The statements, opinions and data contained in all publications are solely those of the individual author(s) and contributor(s) and not of MDPI and/or the editor(s). MDPI and/or the editor(s) disclaim responsibility for any injury to people or property resulting from any ideas, methods, instructions or products referred to in the content.